ISSN 1087-6596, Glass Physics and Chemistry, 2018, Vol. 44, No. 6, pp. 503–510. © Pleiades Publishing, Ltd., 2018.
Original Russian Text © V.Ya. Shevchenko, V.A. Blatov, G.D. Ilyushin, 2018, published in Fizika i Khimiya Stekla.

Cluster Self-Organization of Intermetallic Systems: New 143-Atom Icosahedral Nanocluster-Precursor and the Self-Assembly of a Crystalline Framework $(Ba,Ca)_{46}Li_{102}$ ($R\bar{3}c$, $hR888$)

V. Ya. Shevchenko[a], *, V. A. Blatov[b], and G. D. Ilyushin[b, c]

[a] *Grebenshchikov Institute of Silicate Chemistry, Russian Academy of Sciences, St. Petersburg, 199034 Russia*
[b] *Samara Center for Theoretical Materials Science, Samara State Technical University, Samara, 443100 Russia*
[c] *Federal Research Center Crystallography and Photonics, Russian Academy of Sciences, Moscow, 119333 Russia*
**e-mail: shevchenko@isc.nw.ru*

Received June 8, 2018

Abstract—A combinational-topological analysis of the crystalline structure $(Ba,Ca)_{46}Li_{102}$ ($R\bar{3}c$, $hR888$, V = 30978 Å^3) are performed by computers (the TOPOS software package). The framework-forming the 143-atom icosahedral nanocluster *ico*-K143 with a diameter of 20 Å is established by the method of the complete decomposition of a 3D atomic lattice into cluster structures. *ico*-K143 nanoclusters of a symmetry of $g = \bar{3}$ are shown to be three-layered: Li @12(Li_{12}) @32($Li_{12}Ba_{20}$) @98($Ba_{32}Li_{66}$). The second shell corresponds to the Bergman cluster with 32, 90, and 60 peaks, edges, and faces, respectively. The third new type of icosahedral shell consisting of 98 atoms is characterized by 98, 288, and 192 peaks, edges, and faces, respectively. The chemical composition of the third shell is made up of $Ba_{32}Li_{66}$. In the third shell, 32 Ba atoms were located above all the 32 atoms of the $Li_{12}Ba_{20}$ shell. The symmetry and topological code of the self-assembly of 3D structures from *ico*-K143 nanoclusters-precursors are simulated in the following form: primary chain → layer → framework. The *ico*-K143 nanoclusters formed densely packed 2D layers 3^6 positioned with a shift along the *c* axis. The distance between centers of *ico*-K143 clusters is determined by the translation vector value a_{hex} = 19.913 Å. The large voids in the 3D framework are occupied by 12-atom Ba_3Li_9 clusters with the symmetry $g = 32$.

Keywords: self-assembly of crystalline structures, icosahedral three-layered cluster-precursor Li @12(Li_{12}) @32($Li_{12}Ba_{20}$) @98($Ba_{32}Li_{66}$), structural type $(Ba,Ca)_{46}Li_{102}$-$hR888$

DOI: 10.1134/S1087659618060172

INTRODUCTION

At present, there are several types of two-layered icosahedral clusters known in the chemistry of intermetallics that differ by the number of atoms in the second shell: 1@12@32 (Bergman cluster [1]), 1@12@42 (Mackay cluster [2]), and 1@12@50 [1].

Intermetallics containing Bergman nanoclusters are formed in multiple binary and ternary systems. Up to 150 crystalline structures have been investigated [3]. The chemical composition and structure of binary intermetallics with Bergman nanoclusters-precursors were investigated in [1].

Ternary and binary intermetallics containing local regions in the forms of Bergman icosahedral clusters represent the most complex crystalline structures in terms of crystal chemistry. Table 1 demonstrates intermetallics with a unit cell volume exceeding 10000 Å^3 containing up to 1100 atoms [4–12].

The crystal structure of $(Ba,Ca)_{46}Li_{102}$ ($Li_{33.3}Ba_{13.1}Ca_3$, [12]) exhibits the largest values of the unit cell volume V = 30979 Å^3 and the translation vector c = 90.213 Å (Table 1). The CN values of 15 (for one atom), 16 (for seven atoms), and 17 (for two atoms) were found for 10 crystallographically independent Ba atoms. In the crystal structure of $(Ba,Ca)_{46}Li_{102}$, the Ca atoms are statistically distributed along the crystallographic positions of 8 Ba atoms [12].

The crystal structure of $(Ba,Ca)_{46}Li_{102}$ was described in the form of bonded Li(Li_4Ba_8) icosahedra with Li(Li_{12}) and Li(Li_9Ba_3) icosahedra located between them [12].

The present study carries out a geometrical and topological analysis of the crystal structure of the $(Ba,Ca)_{46}Li_{102}$ intermetallic system by the ToposPro software package [13]. The symmetry and topological code of the process of cluster self-assembly from the

Table 1. Crystal structures with Bergman clusters

Intermetallic	Space group	Pearson coefficient	Unit cell parameters, Å and degrees	V, Å^3	R-factor
$Na_{49}Cd_{58}Sn_{38}$ [4]	$R\,\bar{3}\,m$ (166)	$hR147$	16.034, 16.034, 50.640, 90.00, 90.00, 120.00	11274.8	0.042
$K_{34}In_{90}Zn_{13}$ [5]	$R\,\bar{3}\,m$ (166)	$hR138$	18.439, 18.439, 40.086, 90.00, 90.00, 120.00	11803.3	0.054
$K_{34}In_{91}Mg_{14}$ [5]	$R\,\bar{3}\,m$ (166)	$hR139$	18.750, 18.750, 40.547, 90.00, 90.00, 120.00	12345.0	0.074
$Li_{33}(Cu,Zn)_{11}Al_{56}$ [6]	$P4_2/mmc$ (131)	$tP906$	14.050, 14.050, 83.140, 90.00, 90.00, 90.00	16412.0	0.067
$Li_3Na_5Ga_{20}$ [7]	$Fmmm$ (69)	$oF920$	24.666, 15.974, 45.271, 90.00, 90.00, 90.00	17837.4	0.072
$Mg_{402}Zn_{686}$ [8]	$Cmc2_1$ (36)	$oC1088$	36.840, 22.782, 22.931, 90.00, 90.00, 90.00	19245.7	0.170
$Na_{128}Au_{81}Ga_{275}$ [9]	$Fmmm$ (69)	$oF968$	16.088, 25.584, 46.860, 90.00, 90.00, 90.00	19287.4	0.073
$Li_{13}Na_{29}Ba_{19}$ [10]	$F\,\bar{4}3m$ (216)	$cF488$	27.335, 27.335, 27.335, 90.00, 90.00, 90.00	20424.8	0.048
$BaLi_{1.06}In_{1.16}$ [11]	$R\,\bar{3}\,c$ (167)	$hR888$	18.894, 18.894, 85.289, 90.00, 90.00, 120.00	26367.7	0.061
$(Ba,Ca)_{46}Li_{102}$ [12]	$R\,\bar{3}\,c$ (167)	$hR888$	19.913, 19.913, 90.213, 90.00, 90.00, 120.00	30978.5	0.101

143-atom nanocluster in the form of the primary chain $S_3^1 \rightarrow$ layer $S_3^2 \rightarrow$ framework S_3^3 was established.

This study represents a follow-up of [1, 2, 14–22] in the simulation of processes of self-the assembly of systems on the suprapolyhedral level and the geometric and topological analysis of crystal structures by advanced computer methods.

TECHNIQUES USED IN COMPUTER ANALYSIS

The geometric and topological analysis was carried out by the ToposPro [13] software package that allows performing a multipurpose automated investigation of the crystal structure built on the presentation of structures as "folded graphs" (quotient graphs). The data on the functional role of the atoms at the formation of the crystal structure were obtained by calculating the coordination sequences, i.e., the number sets $\{N_k\}$, where N_k is the number of atoms in the k-coordination sphere of a specific atom.

The obtained values of the coordination sequences of atoms in 3D-lattices are provided in Table 2, where the number of neighboring atoms in the adjacent region, i.e., in the first coordination sphere, are given in bold. All the atoms exhibited various sets of the coordination sequences $\{N_k\}$, so that they are all different topologically (and functionally).

The algorithm of the automated decomposition of any intermetallic structure, represented as a folded graph, on the cluster units was based on the following principles. A structure is formed as a result of the self-assembly from clusters-precursors. Here, the clusters-precursors formed a framework of the structure, where voids were occupied by clusters-spacers (consisting of a small number of atoms). Nanoclusters-precursors did not have shared internal atoms, although shared surface atoms could be observed. The

clusters-precursors occupied highly symmetric positions. A set of nanoclusters-precursors and clusters-spacers consisted of all the atoms of the structure. The algorithm was implemented in the ToposPro software package [13].

SELF-ASSEMBLY OF THE CRYSTAL STRUCTURE OF $(Ba,Ca)_{46}Li_{102}$

The applied method of the simulation of the crystalline structure was based on the determination of the hierarchic sequence of its self-assembly in the crystallographic dimension [14, 15]. At the first level of the system's self-assembly, the mechanism was determined by the formation of the primary chain of the structure from nanoclusters of the 0-level, formed at the template stage of the system's chemical evolution, then the mechanism of self-assembly from the chain of the level was initiated (2nd level) and, thereafter, from the layer a 3D framework of the structure (3rd level) was initiated.

Crystallographic data on $(Ba,Ca)_{46}Li_{102}$. The space group $R\bar{3}c$ is characterized by elements with the point symmetry $g = 32$ (6*a*), $g = -3$ (6*b*), 3 (12*c*), -1 (18*d*), and 2 (18*e*).

Table 2 demonstrates the local surroundings of the Li and Ba atoms and the coordination sequence values in the 3D atomic network.

The number of variations of the decomposition of a 3D atomic lattice with of 3, 4, 5, 6, and 7 structural units equaled 3, 16, 53, 44, and 17 (total 133 variations), respectively.

The variant of describing the crystal structure of $(Ba,Ca)_{46}Li_{102}$ suggested in [12] implying isolation of the layer from the bonded $Li(Li_4Ba_8)$ icosahedra with the $Li(Li_{12})$ and $Li(Li_9Ba_3)$ icosahedra located between them corresponds to the variation with the largest number of elementary structural units of 7 (Table 3). Upon the selection of such a type of intermetallics simulation, apart from the three investigated elementary polyhedral clusters, the functional role of another three isolated elementary polyhedral clusters (Ba1(1)(1@16), Li3(1)(1@12), and Ba4(1)(1@17)) and atoms-spacers (Li5(0)(1)) must be considered.

Quasis-pherical clusters the *ico*-K143 of $Li(Li_{12})(Li_{12}Ba_{20})(Ba_{32}Li_{66})$ composition, Ba_3Li_9 clusters-spacers, and Li atoms-spacers were established as the framework-forming nanoclusters (Table 4, Figs. 1, 2).

The *ico*-K143 nanocluster appeared to be three-layered of composition 1@12@32@98 with the center in the position 6*b* (1/3, 2/3, 1/6) and the point symmetry $g = -3$.

Table 2. Local surroundings of Li, Ba atom and coordination sequence values

Atom	Local surrounding	Coordination sequences				
		N_1	N_2	N_3	N_4	N_5
Li6	12Li	**12**	32	97	193	328
Li1	12Li	**12**	32	98	198	338
Li2	9Li + 3Ba	**12**	43	112	211	367
Li3	8Li + 4Ba	**12**	45	112	221	342
Li8	8Li + 4Ba	**12**	45	114	217	342
Li14	8Li + 4Ba	**12**	46	108	220	351
Li9	7Li + 5Ba	**12**	48	108	215	357
Li17	7Li + 5Ba	**12**	48	111	220	357
Li5	7Li + 5Ba	**12**	48	112	218	361
Li11	7Li + 5Ba	**12**	48	116	212	367
Li4	7Li + 5Ba	**12**	48	118	216	344
Li16	7Li + 5Ba	**12**	48	118	225	359
Li15	7Li + 5Ba	**12**	48	119	220	362
Li7	7Li + 5Ba	**12**	48	123	222	346
Li10	7Li + 5Ba	**12**	49	122	227	359
Li13	6Li + 6Ba	**12**	51	129	235	365
Li12	6Li + 6Ba	**12**	52	129	238	360
Li19	4Li + 8Ba	**12**	56	130	233	372
Li18	4Li + 8Ba	**12**	57	131	224	357
Ba3	8Li + 7Ba	**15**	61	130	243	383
Ba2	12Li + 4Ba	**16**	52	112	220	361
Ba1	12Li + 4Ba	**16**	52	112	219	367
Ba6	11Li + 5Ba	**16**	55	129	240	368
Ba10	11Li + 5Ba	**16**	56	121	224	366
Ba9	11Li + 5Ba	**16**	56	123	232	371
Ba7	11Li + 5Ba	**16**	56	124	232	372
Ba8	10Li + 6Ba	**16**	58	134	243	380
Ba4	12Li + 5Ba	**17**	56	118	216	391
Ba5	12Li + 5Ba	**17**	57	119	236	371

Table 3. Variations of cluster representation of crystal structure. Displayed: central atoms of polyhedral cluster (Li and Ba) and total number of shells (first braces) and number of atoms in shells (second braces)

Three structural units
Li1(3)(1@12@32@98) Li2(0)(1) Li3(1)(1@12)
Li1(3)(1@12@32@98) Li2(0)(1) Li16(1)(1@12)
Li1(1)(1@12) Li2(2)(1@12@43) Li9(1)(1@12)
Four structural units
Li1(2)(1@12@32) Li2(1)(1@12) Li3(1)(1@12) Ba9(1)(1@16)
Li1(2)(1@12@32) Li2(1)(1@12) Li9(1)(1@12) Li16(1)(1@12)
Li1(2)(1@12@32) Li2(1)(1@12) Li15(1)(1@12) Li17(1)(1@12)
Li1(2)(1@12@32) Li2(1)(1@12) Li15(1)(1@12) Ba9(1)(1@16)
Li1(1)(1@12) Li3(1)(1@12) Li9(1)(1@12) Li12(1)(1@12)
Li1(2)(1@12@32) Li3(1)(1@12) Li12(1)(1@12) Ba9(1)(1@16)
Li1(1)(1@12) Li9(1)(1@12) Li12(1)(1@12) Li15(1)(1@12)
Li1(1)(1@12) Li9(1)(1@12) Li12(1)(1@12) Li16(1)(1@12)
Li1(1)(1@12) Li9(1)(1@12) Li13(1)(1@12) Li15(1)(1@12)
Li1(1)(1@12) Li9(1)(1@12) Li13(1)(1@12) Li16(1)(1@12)
Li1(2)(1@12@32) Li12(1)(1@12) Li15(1)(1@12) Li17(1)(1@12)
Li1(2)(1@12@32) Li12(1)(1@12) Li15(1)(1@12) Ba9(1)(1@16)
Li1(2)(1@12@32) Li13(1)(1@12) Li15(1)(1@12) Li17(1)(1@12)
Li1(1)(1@12) Li2(2)(1@12@43) Ba4(0)(1) Li5(1)(1@12)
Li1(1)(1@12) Ba1(2)(1@16@52) Li3(1)(1@12) Ba7(0)(1)
Li1(0)(1) Ba1(2)(1@16@52) Li3(1)(1@12) Ba7(1)(1@16)
Seven structural units
Li1(0)(1) Li2(1)(1@12) Ca2(1)(1@16) Li3(1)(1@12) Ba4(1)(1@17) Li17(0)(1) Li18(1)(1@12)
Li1(0)(1) Li2(0)(1) Ca2(1)(1@16) Li3(1)(1@12) Ba4(0)(1) Li17(1)(1@12) Li18(1)(1@12)
Li1(0)(1) Li2(1)(1@12) Ca2(1)(1@16) Li3(0)(1) Ba4(1)(1@17) Li17(1)(1@12) Li18(1)(1@12)
Li1(0)(1) Li2(0)(1) Ca2(1)(1@16) Li3(1)(1@12) Ba4(1)(1@17) Li17(1)(1@12) Li18(1)(1@12)
Li1(0)(1) Li2(1)(1@12) Ca2(1)(1@16) Li3(1)(1@12) Ba4(1)(1@17) Li17(0)(1) Ba7(1)(1@16)
Li1(0)(1) Li2(0)(1) Ca2(0)(1) Li3(1)(1@12) Ba4(0)(1) Li17(1)(1@12) Ba7(1)(1@16)
Li1(0)(1) Li2(0)(1) Ca2(0)(1) Li3(0)(1) Ba4(1)(1@17) Li17(1)(1@12) Ba7(1)(1@16)
Li1(1)(1@12) Li2(1)(1@12) Ba1(1)(1@16) Li3(1)(1@12) Ba4(1)(1@17) Li5(0)(1) Li18(1)(1@12)
Li1(1)(1@12) Li2(0)(1) Ba1(1)(1@16) Li3(1)(1@12) Ba4(1)(1@17) Li5(0)(1) Li18(1)(1@12)
Li1(0)(1) Li2(0)(1) Ba1(1)(1@16) Li3(1)(1@12) Ba4(0)(1) Li5(1)(1@12) Li18(1)(1@12)
Li1(0)(1) Li2(1)(1@12) Ba1(1)(1@16) Li3(0)(1) Ba4(1)(1@17) Li5(1)(1@12) Li18(1)(1@12)

Table 4. Atoms forming icosahedral cluster 1@12 and 32-, 98-atom shells

Icosahedral cluster 1@12	32-atom shell		98- atom shell	
1 Li1	6 Ba10	6 Li18	2 Ba1	6 Li11
6 Li10	6 Ba5	6 Li5	6 Ba4	6 Li12
6 Li4	6 Ba7		12 Ba6	6 Li13
	2 Ba2		6 Ba8	6 Li14
			6 Ba9	6 Li15
				6 Li17
				6 Li19
				6 Li6
				6 Li7
				6 Li8
				6 Li9

The center of the Ba_3Li_9 cluster-spacer with the point symmetry $g = 32$ was located in the position 6*a* (2/3, 1/3, 0.583) (Fig. 1).

The second 32-atom icosahedral shell-deltohedron corresponded to the Bergman cluster with 32, 90, and 60 peaks, edges, and faces, respectively (Fig. 2). The second shell contained 20 Ba atoms located on 20 edges of an icosahedron and 12 Li atoms bonded to 12 Li atoms (peaks of the icosahedrons).

The third new type of 98-atom icosahedral shell-deltohedron exhibited of 98, 288, and 192 peaks, edges, and faces. The chemical composition of the shell

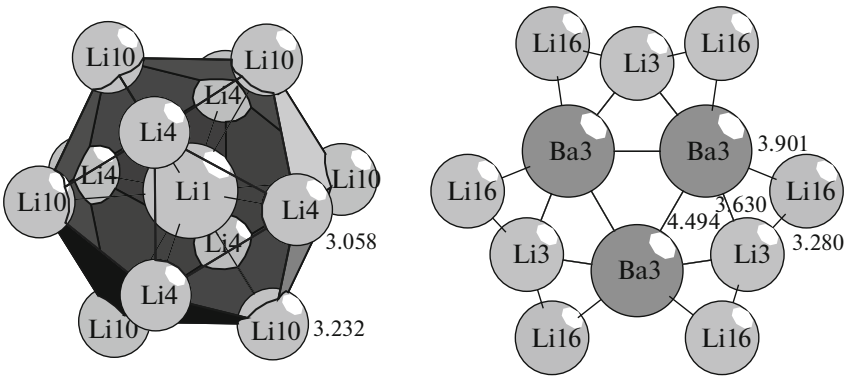

Fig. 1. Li(Li_{12}) cluster (left) and Li_9Ba_3 cluster (right). Numbers indicate distances of atomic bonds, Å.

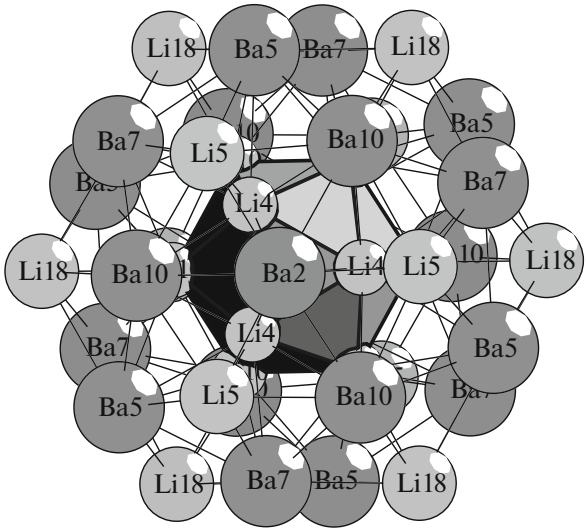

Fig. 2. Two-layer Li @12(Li_{12}) @32($Li_{12}Ba_{20}$) cluster.

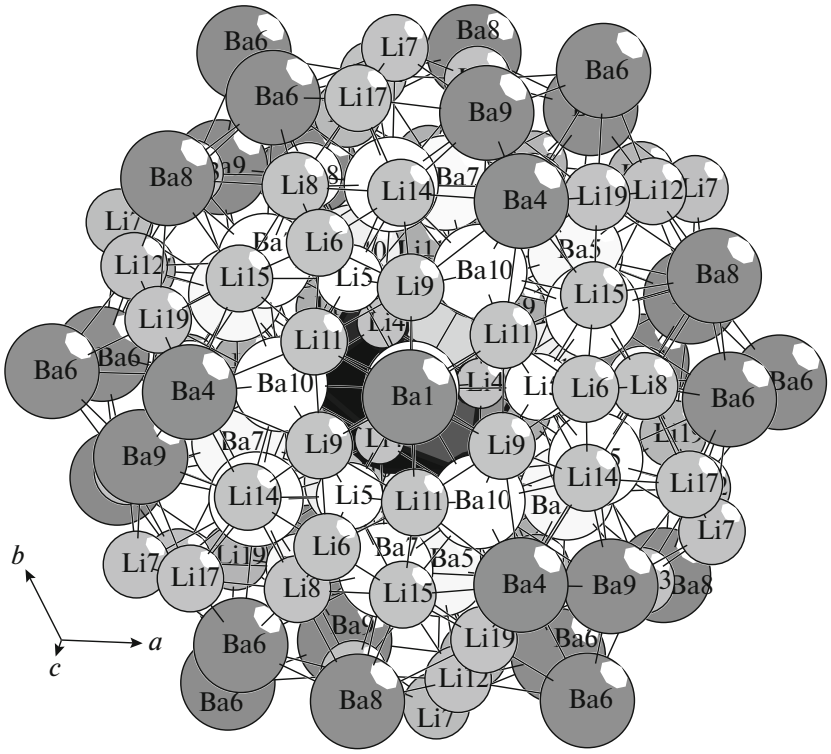

Fig. 3. Three-layer Li @12(Li_{12}) @32($Li_{12}Ba_{20}$) @98($Ba_{32}Li_{66}$) cluster.

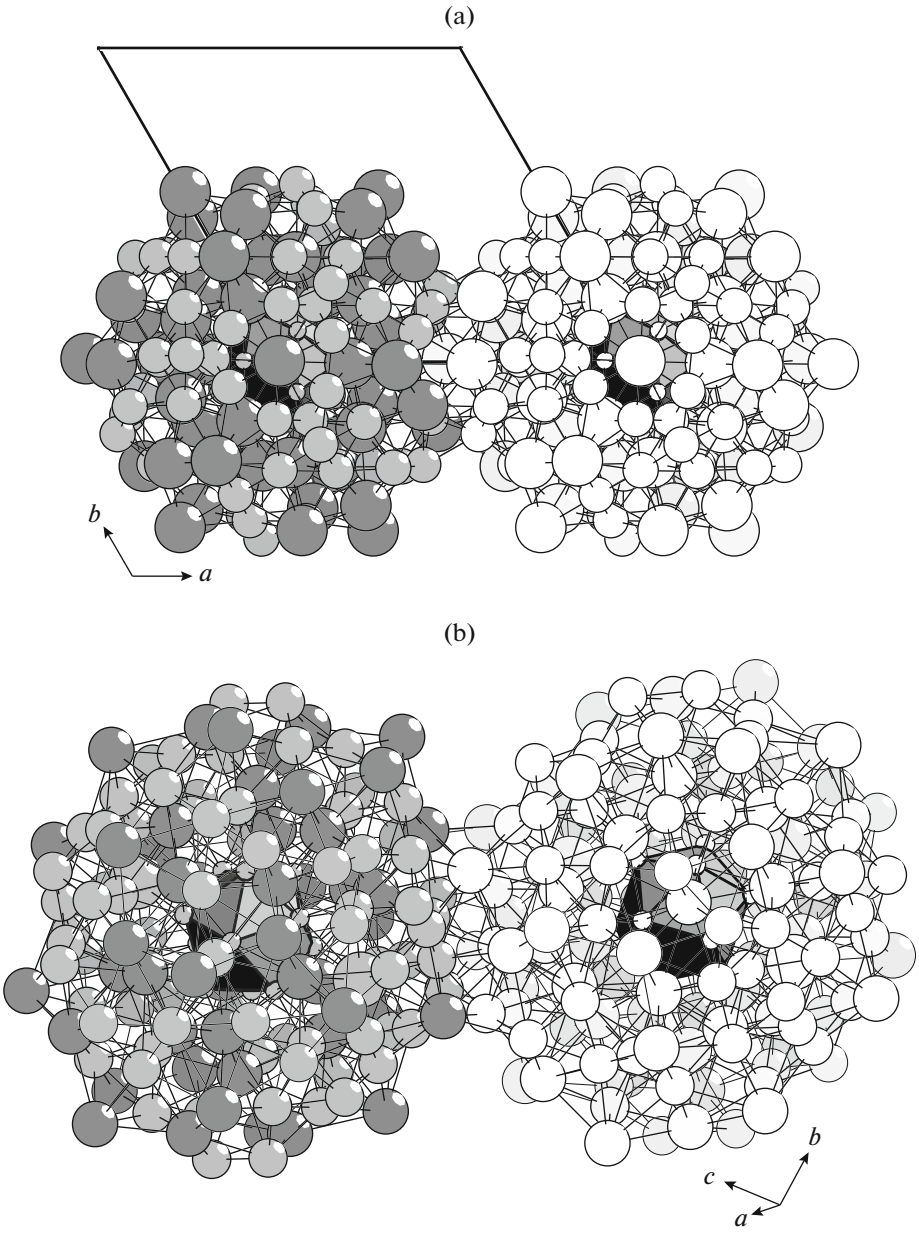

Fig. 4. (a) Mechanism of *ico*-K143 clusters bonding upon formation of primary chain and layer, (b) mechanism of clusters *ico*-K143 bonding from adjacent layers upon formation of framework.

is Ba_{32} Li_{66}. In the third shell, all 32 Ba atoms were located above 32 atoms of the Berman shell (Fig. 3).

The basic 3D lattice for the framework-forming *ico*-K143 clusters corresponded to the hexagonal densest packing of clusters with CN = 12 = 6 (in the layer) + 3 (above the layer) + 3 (under the layer).

Self-assembly of the $(Ba,Ca)_{46}Li_{102}$ *crystalline structure*. *Primary chain*. The self-assembly of the primary chains from the *ico*-K143 cluster proceeded along the *X* axis (Fig. 4). Here, the localization of two atoms-spacers (Li2) occurred between *ico*-K143 clusters.

The distance between the centers of *ico*-K143 clusters corresponds to the translation vector value a = 19.913 Å.

Self-assembly of the layer. The formation of the S_3^2 layer proceeded upon the complementary bonding of the clusters from the adjacent primary chains with a shift (Fig. 5). At this stage of self-assembly, localization occurs in the voids of the Ba_3Li_9 cluster-spacer.

The distance between the centers of *ico*-K143 clusters from the adjacent primary chains corresponded to the translation vector value b = 19.913 Å.

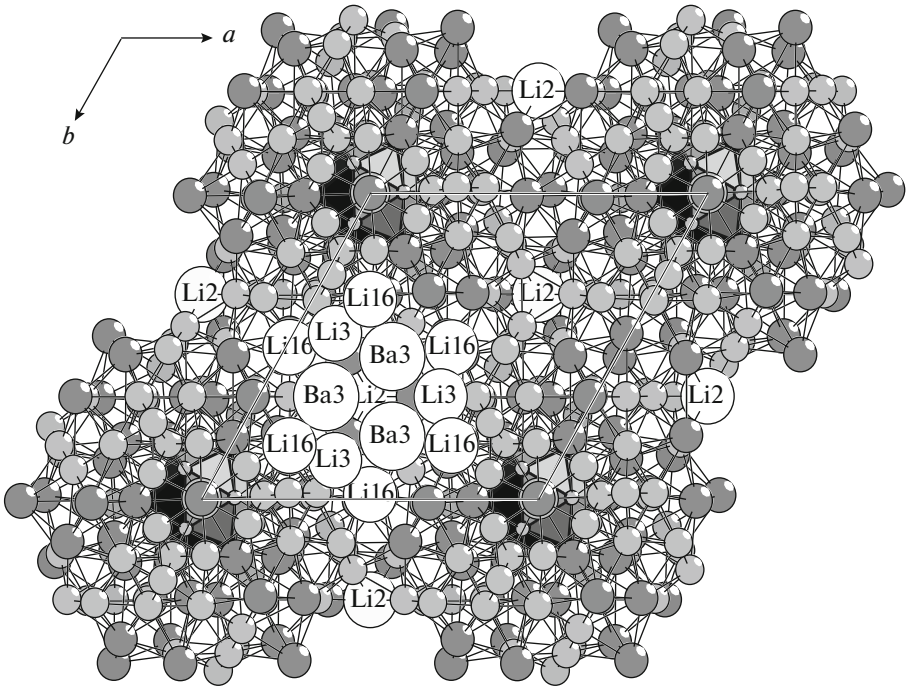

Fig. 5. Layer of two primary chains. Ba_3Li_9 clusters-spacers and Li atoms-spacers are displayed.

Self-assembly of the framework. The structure of the framework of S_3^3 is formed upon the bonding of two basic layers with a shift. The distance between layers along the Z axis determines the translation vector value $c/6 = 90.213$ Å/6.

CONCLUSIONS

The framework-forming 143-atom icosahedral nanocluster with a diameter of 20 Å has been established via the method of the complete decomposition of the 3D atomic lattice into cluster structures. *ico*-K143 nanoclusters have been determined as three-layered Li @12(Li_{12}) @32($Li_{12}Ba_{20}$) @98($Ba_{32}Li_{66}$) with a symmetry of $g = \overline{3}$.

The symmetrical and topological code of the self-assembly processes of 3D structures from *ico*-K143 nanoclusters-precursors in the primary chain → layer → framework form has been reconstructed. *ico*-K143 nanoclusters form densely packed 2D layers 3^6 located with a shift along the *c* axis.

The 12-atom Ba_3Li_9 clusters-spacers with a symmetry of $g = 32$ that occupied voids in the 3D framework structure and Li atoms-spacers that participated in the bonding of *ico*-K143 upon the formation of the primary chain and layer have been identified.

ACKNOWLEDGMENTS

This study was supported by the Russian Foundation for Basic Research (project no. 16-12-00105) and the Federal Agency for Scientific Organizations (agreement no. 007-GZ/ChZ3363/26).

REFERENCES

1. Akhmetshina, T.G. and Blatov, V.A., A Bergman, Bergman-based and 63-atom nanoclusters in intermetallics, *Struct. Chem.,* 2016, vol. 27, pp. 1685–1692.
2. Akhmetshina, T.G. and Blatov, V.A., A fascinating building unit: Mackay cluster in intermetallics, *Struct. Chem.,* 2017, vol. 28, pp. 133–140.
3. Villars P., Cenzual K., *Pearson's Crystal Data-Crystal Structure Database for Inorganic Compounds (PCDIC),* Materials Park, OH: ASM International, 2010.
4. Todorov, E. and Sevov, S.C., Synthesis, characterization, electronic structure, and bonding of heteroatomic deltahedral clusters: $Na_{49}Cd_{58.5}Sn_{37.5}$, A network structure containing the first empty icosahedron without a group 13 element and the largest *closo*-deltahedron, *J. Am. Chem. Soc.,* 1997, vol. 119, pp. 2869–2876.
5. Li, B. and Corbett, J.D., Electronic stabilization effects: Three new K–In–T (T = Mg, Au, Zn) network compounds, *Inorg. Chem.,* 2006, vol. 45, pp. 8958–8964.
6. Leblanc, M., Le Bail, A., and Audier, M., Crystalline phases related to the icosahedral Al–Li–Cu phase: A single crystal X-ray diffraction study of the tetragonal τ-$Al_{56}(Cu,Zn)_{11}Li_{33}$ phase, *Phys. B (Amsterdam, Neth.),* 1991, vol. 173, pp. 329–355.

7. Charbonnel, M. and Belin, C., Synthesis and crystal structure of the new nonstoichiometric phase $Li_3Na_5Ga_{19.56}$, *Nouv. J. Chim.,* 1984, vol. 8, pp. 595–599.
8. Kreiner, G., Towards realistic quasiperiodic structures: Modelling, synthesis and structure of $(Ga,Zn)_{175-\delta}Mg_{97+\delta}$—A large 3/2-2/1-2/1 Fibonacci approximant, *J. Alloys Compd.,* 2002, vol. 338, pp. 261–273.
9. Tillard-Charbonnel, M., Belin, C., and Chouaibi, N., Crystal structure of sodium gold gallium, $Na_{128}Au_{81}Ga_{275}$, *Z. Kristallogr.,* 1993, vol. 206, pp. 310–312.
10. Smetana, V., Babizhetskyy, V., Vajenine, G., and Simon, A., Neue Li_{26}-cluster in $Li_{13}Na_{29}Ba_{19}$, *Z. Anorg. Allg. Chem.,* 2006, vol. 632, pp. 2115–211.
11. Smetana, V., Vajenine, G.V., Kienle, L., Duppel, V., and Simon, A., Intermetallic and metal-rich phases in the system Li–Ba–In–N, *J. Solid State Chem.,* 2010, vol. 183, no. 8, pp. 1767–1775.
12. Smetana, V., Babizhetskyy, V., Hoch, C., and Simon, A., Icosahedral Li clusters in the structures of $Li_{33.3}Ba_{13.1}Ca_3$ and $Li_{18.9}Na_{8.3}Ba_{15.3}$, *J. Solid State Chem.,* 2007, vol. 180, pp. 3302–3309.
13. Blatov, V.A., Shevchenko, A.P., and Proserpio, D.M., Applied topological analysis of crystal structures with the program package ToposPro, *Cryst. Growth Des.,* 2014, vol. 14, no. 7, pp. 3576–3585. http://topospro.com/.
14. Ilyushin, G.D., *Modelirovanie protsessov samoorganizatsii v kristalloobrazuyushchikh sistemakh* (Modeling of Self-Organization Processes in Crystal Forming Systems), Moscow: Editorial URSS, 2003.
15. Ilyushin, G.D., Theory of cluster self-organization of crystal-forming systems. geometrical-topological modeling of nanocluster precursors with a hierarchical structure, *Struct. Chem.,* 2012, vol. 20, no. 6, pp. 975–1043.
16. Pankova, A.A., Blatov, V.A., Ilyushin, G.D., and Proserpio, D.M., γ-Brass polyhedral core in intermetallics: The nanocluster model, *Inorg. Chem.,* 2013, vol. 52, no. 22, pp. 13094–13107.
17. Shevchenko, V.Ya., Blatov, V.A., and Ilyushin, G.D., Symmetry and topology codes of cluster self-assembly for icosahedral structures of the $NaZn_{13}$-*cF*112 and TRB_{66}-*cF*1944 family, *Glass Phys. Chem.,* 2015, vol. 41, no. 4, pp. 341–351.
18. Shevchenko, V.Ya., Blatov, V.A., and Ilyushin, G.D., Modeling of self-organization processes in crystal-forming systems: Symmetry and topological codes of cluster self-assembly of a 2D layered icosahedral structure of $Sc_{18}B_{238}$ (*Pbam*, *oP*514), *Glass Phys. Chem.,* 2016, vol. 42, no. 3, pp. 221–229.
19. Shevchenko, V.Ya., Blatov, V.A., and Ilyushin, G.D., The symmetric and topological code of the cluster self-assembly of the crystal structure of ε-$Mg_{23}Al_{30}$ of K63 nanoclusters, *Glass Phys. Chem.,* 2017, vol. 43, no. 6, pp. 512–520.
20. Blatov, V.A., Ilyushin, G.D., and Proserpio, D.M., Nanocluster model of intermetallic compounds with giant unit cells: β,β'-Mg_2Al_3 polymorphs, *Inorg. Chem.,* 2010, vol. 49, no. 4, pp. 1811–1818.
21. Shevchenko, V.Ya., Blatov, V.A., and Ilyushin, G.D., Intermetallic compounds of the $NaCd_2$ family perceived as assemblies of nanoclusters, *Struct. Chem.,* 2009, vol. 20, no. 6, pp. 975–982.
22. Blatov, V.A. and Ilyushin, G.D., New method for computer analysis of complex intermetallic compounds and nanocluster model of the samson phase Cd_3Cu_4, *Crystallogr. Rep.,* 2010, vol. 55, no. 7, pp. 1100–1105.

Translated by D. Marinin